Proceedings of *RAGtime 20–22, 15–19 Oct., 16–20 Sept., 19–23 Oct., 2018/2019/2020, Opava, Czech Republic*
Z. Stuchlík, G. Török and V. Karas, editors, Silesian University in Opava, 2020, pp. 257–262

On maximum energy cutoff in the hotspot of radiogalaxies 3C 105 and 3C 445

Yelyzaveta Pulnova[1,2,a] and Anabella Araudo[2,3,b]

[1]Institute of Theoretical Physics, Faculty of Mathematics & Physics, Charles University, V Holešovıckách 2/747, Prague, Czech Republic
[2]ELI Beamlines, Institute of Physics, Czech Academy of Sciences, 25241 Dolní Břežany, Czech Republic
[3]Astronomical Institute, Czech Academy of Sciences, Boční II 1401, CZ-141 00 Prague, Czech Republic
[a]Yelyzaveta.Pulnova@eli-beams.eu
[b]Anabella.Araudo@eli-beams.eu

ABSTRACT
The origin of Ultra-High-Energy Cosmic Rays is still unknown, and Active Galactic Nuclei have been proposed as candidates to accelerate these particles. Using the well-resolved radio emission from radiogalaxies 3C 105 and 3C 445 we investigate the standard assumption that the distribution of non-thermal electrons has a maximum energy cutoff due to the synchrotron cooling. We show that as a consequence this would lead to an unphysically large number density in the hotspot. This result has important implications for the origin of Ultra-High-Energy Cosmic Rays.

Keywords: Ultra-high-energy cosmic rays – diffusive shock acceleration –synchrotron cooling

1 INTRODUCTION

Ultra-high-energy cosmic rays (UHECR) are charged particles detected on Earth with energy higher than 10^{18} eV. The origin of these particles is still unknown. The very upper limit to the maximum achievable energy was estimated by Hillas (1984) by assuming that the maximum displacement of a charged particle by an electric field is the size of the system L. The Hillas energy, or the maximum energy achievable by a particle with charge Zq, is

$$E_{\mathrm{Hillas}} = \frac{L}{ZqB}\left(\frac{v}{c}\right) \sim 10^{18}\left(\frac{v}{c}\right)\left(\frac{L}{\mathrm{kpc}}\right)\left(\frac{B}{100\mu\mathrm{G}}\right)^{-1}\ \mathrm{eV}, \tag{1}$$

where B is the magnetic field and v the velocity of the plasma. We see that for compact objects a strong magnetic field is required, while for a weak field the source should be extended enough. White dwarfs, active galactic nuclei, galaxy clusters, and radio galaxies

978-80-7510-433-5

Table 1. From left to right, we list the name of the source, the redshift (z), the scale (in kpc arcsec^{-1}), the distance (in Gpc), the radio spectral index α, the steepness of the relativistic electrons energy distribution $s = 2\alpha + 1$, and the proton to electron energy density ratio a.

Source	z	scale	d	α	s	a
3C 105	0.089	1.642	0.4017	0.8	2.6	4.51
3C 445	0.0562	1.077	0.2479	0.75	2.5	6.58

are candidates to accelerate UHECRs. In this work, we study the hotspots in the termination region of radiogalaxy jets.

Araudo et al. (2016) [A16] showed that the maximum energy of particles accelerated in the hotspots of FR II radiogalaxies is $\sim$ 10 TeV, and therefore much smaller than the energy of UHECRs. Based on theoretical and observational constraints, and for a sample of sources (3C 105, 3C 195, 3C 227, 3C 403, and 3C 445), [A16] demonstrated that at least the plasma density is unreasonably large, hotspots cannot accelerate UHECRs. In the present contribution, we consider the southern hotspots in 3C 105 and 3C 445.but considering the substructures in the hotspots.

2 THE CASES STUDY 3C 105 S AND 3C 445 S

We select the southern hotspots in radioagalaxies 3C 105 and 3C 445 from where high resolution radio data taken with the Very Large Array (VLA) are available in the literature. Parameters used for the analysis are listed in Table 1.

3C 105 South

Radiogalaxy 3C 105 is located at redshift $z = 0.089$. At radio frequencies (8.4 GHz), three knots denoted on Fig. 1 as S1, S2, and S3 are resolved in the southern hotspot (Migliori et al., 2020).

3C 445 South

Radiogalaxy 3C 445 is located at redshift $z = 0.05623$. The southern hotspot 3C 445 South has two components at 22 GHz, denoted as SE and SW for Eastern and Western knot, respectively (Orienti et al., 2020). SE is well-resolved and sufficiently larger and brighter than the SW knot. The latter has a compact radio-loud part and is surrounded by the large cloud of the radio fainter emitting matter, which is neglected in our analysis.

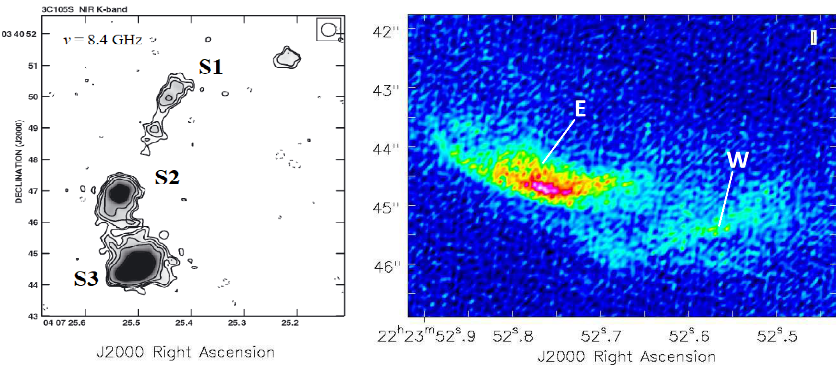

Figure 1. *Left:* Southern hotspot of radiogalaxy 3C 105 at 8.4 GHz. The three knots are denoted as S1, S2 and S3. Credit: Mack et al. (2009). *Right:* The hotspot complex 3C 445 South at 22 GHz. Eastern and Western components are denoted as E, W, respectively. Credit: Orienti et al. (2020)

3 EQUIPARTITION MAGNETIC FIELD

We estimate the intensity of the magnetic field separately for every knot of the hotspot. By assuming equipartition between the non-thermal electron and magnetic energy densities, which means $U_{e,\mathrm{NT}} = U_{\mathrm{mag}}$, we obtain

$$\frac{B_{e,\mathrm{eq}}^2}{8\pi} = U_{e,\mathrm{NT}} = \int_{E_{e,\mathrm{min}}}^{E_{e,\mathrm{max}}} E N_e(E_e) \mathrm{d}E_e \propto B_{e,\mathrm{eq}}^{-\frac{s+1}{2}}, \tag{2}$$

where $N_e = K_e(s) E_e^{-s}$ is the power-law energy distribution of the non-thermal electrons and $E_{e,\mathrm{min}}$ and $E_{e,\mathrm{max}}$ are the minimum and maximum energies of the electron distribution. Note that $s > 2$ in all the sources in our sample, and therefore most of the energy is contained in the low-energy part of N_e. We assume $E_{e,\mathrm{min}} = 50 m_e c^2$.

To include protons in our calculations we consider that the energy density in non-thermal protons is $U_p = a U_e$, where $a = (m_p/m_e)^{(3-s)/2}$, m_e and m_p are the electron and proton mass, respectively. Then the total equipartition magnetic field can be determined from $B_{\mathrm{eq}} = \sqrt{1+a} B_{\mathrm{eq,e}}$, given

$$B_{\mathrm{eq}} = \xi(s) \left(\frac{\epsilon_{\mathrm{syn},\nu}}{10^{-34}\ \mathrm{erg\ s^{-1}\ cm^{-3}\ Hz^{-1}}} \right)^{\frac{2}{s+5}} \left(\frac{\nu}{\mathrm{GHz}} \right)^{\frac{s-1}{s+5}} \mu\mathrm{G} \tag{3}$$

where $\epsilon_{\mathrm{syn},\nu} = 4\pi d^2 S_\nu V^{-1}$ is synchrotron emissivity per unit frequency, ν is the observed frequency. Constant $\xi(s)$ in case of 3C 105 corresponds to value 96, and 106 otherwise. To calculate the volume V of the emitting regions at the given observed frequency, from Fig. 1 we estimate the minor axis l_{min} and areas of each knot of the hotspots. In Table 2 we list the values of l_{min}, V, and B_{eq} for all the sources in our sample.

Table 2. Observed and derived parameters of the hotspots. From left to right, we list the name of the source and the non-thermal component in the hotspot, the observed frequency ν and measured flux density S_ν, the projected size S and the minor axis $l_{\rm min}$, the volume V, the equipartition magnetic field $B_{\rm eq}$ and $n_{\rm min}$ (see Eq. 7).

Source	Comp.	ν [GHz]	S_ν [mJy]	S [$''\times''$]	$l_{\rm min}$ [kpc]	V [kpc^3]	$B_{\rm eq}$ [μG]	$n_{\rm min}$ [cm^{-3}]
3C 105	S1	8.4	18.4	1.30×0.59	0.97	1.052	198	0.61
	S2	8.4	372	1.68×0.94	1.54	3.422	267	450
	S3	8.4	260	2.20×1.20	1.98	7.387	198	184
3C 445	SE	22	14.24	2.63×0.91	0.51	0.201	229	0.44
	SW	22	2.92	1.02×0.15	0.08	0.002	512	0.83

4 SYNCHROTRON COOLING AND THE PLASMA NUMBER DENSITY

Hotspots in the termination shocks in radiogalaxy jets show a cutoff of the synchrotron spectrum in the optical-IR band, i.e. at $\nu_{\rm c} \sim 10^{13} - 10^{15}$ Hz. From the cutoff of the synchrotron spectrum we estimate the maximum energy of accelerated electrons Lang (2013)

$$E_{e,\rm max} = m_e c^2 \sqrt{\frac{4\pi m_e c}{3q}} \sqrt{\frac{\nu_c}{B}} \sim 0.3 \left(\frac{\nu_{\rm c}}{10^{14}\,{\rm Hz}}\right)^{0.5} \left(\frac{B}{100\,\mu{\rm G}}\right)^{-0.5} {\rm TeV}. \tag{4}$$

It is commonly assumed in the literature that $E_{e,\rm max}$ is determined by synchrotron cooling (Prieto et al., 2002), with a timescale $t_{\rm synchr} \sim 450/(E_{e,\rm max}B^2)$. By equating $t_{\rm acc} = t_{\rm synchr}$, where $t_{\rm acc} = 20D/v_{\rm sh}^2$ is the acceleration time via diffusive shock acceleration, we obtain that the diffusion coefficient is

$$D_{s,c} = 30.7 \frac{v_{\rm sh}^2}{E_{e,\rm max}B^2} = 6.8\times10^{30} \left(\frac{v_{\rm sh}}{c}\right)^2 \left(\frac{\nu_{\rm c}}{10^{14}\,{\rm Hz}}\right)^{-0.5} \left(\frac{B}{100\,\mu{\rm G}}\right)^{-1.5} {\rm cm^2\,s^{-1}}. \tag{5}$$

We assume the shock velocity $v_{\rm sh} = c/3$ in our calculations.

The diffusion coefficient is defined as $D = \lambda c/3$, where $\lambda = r_g^2/s$ is the mean-free path in the small scale diffusion regime, $r_{\rm g}$ is the mean-free path, and s is the scale-length of the magnetic turbulence. The minimum value of s is the ion skin depth $c/\omega_{\rm pi}$. Therefore, by considering $s = c/\omega_{\rm pi}$ we obtain that the maximum value of the diffusion coefficient is

$$D_{\rm max} = \frac{1}{3} r_g^2 \omega_{\rm pi} = 3\times10^{28} \left(\frac{\nu_{\rm c}}{10^{14}\,{\rm Hz}}\right) \left(\frac{n}{\rm cm^{-3}}\right)^{0.5} \left(\frac{B}{100\,\mu{\rm G}}\right)^{-3} {\rm cm^2\,s^{-1}}. \tag{6}$$

If $E_{e,\rm max}$ is determined by synchrotron cooling, then the condition $D_{s,c} < D_{\rm max}$ needs to be satisfied. By following the procedure described in [A16], we determine the minimum

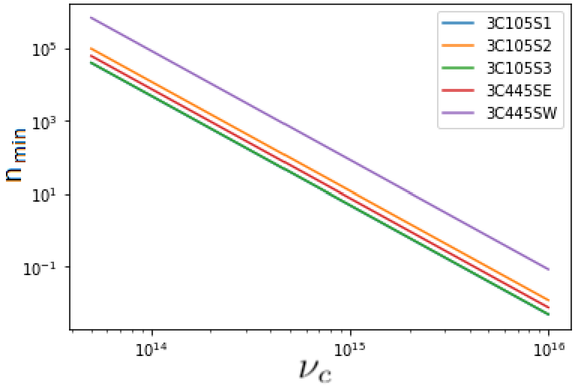

Figure 2. The log-log plot of a lower limit of the number density $n_{\rm min}$ for the cutoff frequencies ν_c in the vicinity of typical values. We use $B = B_{\rm eq}$. Curves from sources 3C 105 S1 and 3C 105 S3 are overlapping.

plasma density in the hotspot to satisfy the condition $D_{s,c} = D_{\rm max}$ giving

$$n_{\rm min} = 5.3 \times 10^4 \left(\frac{v_{\rm sh}}{c}\right)^4 \left(\frac{\nu_{\rm c}}{10^{14}\,\rm Hz}\right)^{-3} \left(\frac{B}{100\,\mu\rm G}\right)^3 \rm cm^{-3}. \tag{7}$$

In Fig. 2 we plot $n_{\rm min}$ as a function of the cutoff frequency ν_c. We chose the vicinity of the typical cutoff frequencies $\nu_c \sim 10^{14} - 10^{15}$ Hz (Orienti et al., 2012)). The values we obtained are far above the typical range of values for the hotspots number density.

5 CONCLUSIONS

Our calculations indicate that electron's maximum energy might not be determined by synchrotron cooling because this assumption leads to unreasonably large values of the lower limit for the plasma number density $n_{\rm min}$ (see Tab. 2). For comparison upper limit for plasma number density in Cyg A and 3C 475 is $n \sim 10^{-4}\rm cm^{-3}$ (Dreher et al., 1987).

Araudo et al. (2016) and Araudo et al. (2018) proposed that electrons maximum energy cutoff in the hotspots of radiogalaxies is due to escape downstream of a quasi-perpendicular shock. In this case, the maximum energy of protons is $E_{p,\rm max} = E_{e,\rm max}$. In this context, the maximum achievable energy of protons in the hotspot of the radiogalaxies 3C 105 S and 3C 445 S is $E_{p,\rm max} \sim$ TeV and therefore these hotspots can not accelerate UHECR. In a more general context, Bell et al. (2018) showed that relativistic shocks are unable to accelerate UHECRs.

ACKNOWLEDGEMENTS

Y.P. thanks ELI Beamlines for the financial support under the project LM2018141. A.T.A. thanks the Czech Science Foundation under the grant GAČR 20-19854S titled "Particle Acceleration Studies in Astrophysical Jets".

REFERENCES

Araudo, A. T., Bell, A. R., Blundell, K. M. and Matthews, J. H. (2018), On the maximum energy of non-thermal particles in the primary hotspot of cygnus a, *Monthly Notices of the Royal Astronomical Society*, **473**(3), pp. 3500–3506.

Araudo, A. T., Bell, A. R., Crilly, A. and Blundell, K. M. (2016), Evidence that the maximum electron energy in hotspots of FR II galaxies is not determined by synchrotron cooling, *Monthly Notices of the Royal Astronomical Society*, **460**(4), pp. 3554–3562.

Bell, A. R., Araudo, A. T., Matthews, J. H. and Blundell, K. M. (2018), Cosmic-ray acceleration by relativistic shocks: Limits and estimates, *Monthly Notices of the Royal Astronomical Society*, **473**(2), pp. 2364–2371, ISSN 13652966.

Dreher, J., Carilli, C. and Perley, R. (1987), The faraday rotation of cygnus a-magnetic fields in cluster gas, *The Astrophysical Journal*, **316**, pp. 611–625.

Hillas, A. M. (1984), The origin of ultra-high-energy cosmic rays, *Annual review of astronomy and astrophysics*, **22**, pp. 425–444.

Lang, K. R. (2013), *Astrophysical Formulae: Space, time, matter and cosmology*, Springer.

Mack, K.-H., Prieto, M., Brunetti, G. and Orienti, M. (2009), Near-infrared/optical counterparts of hotspots in radio galaxies, *Monthly Notices of the Royal Astronomical Society*, **392**(2), pp. 705–717.

Migliori, G., Orienti, M., Coccato, L., Brunetti, G., D'Ammando, F., Mack, K. H. and Prieto, M. A. (2020), Particle acceleration in low-power hotspots: modelling the broad-band spectral energy distribution, *Monthly Notices of the Royal Astronomical Society*, **495**(2), pp. 1593–1607.

Orienti, M., Migliori, G., Brunetti, G., Nagai, H., D'Ammando, F., Mack, K.-H. and Prieto, M. A. (2020), Jansky VLA observations of synchrotron emitting optical hotspots of 3C 227 and 3C 445 radio galaxies, *Monthly Notices of the Royal Astronomical Society*, **494**(2), pp. 2244–2253, ISSN 0035-8711.

Orienti, M., Prieto, M. A., Brunetti, G., Mack, K.-H., Massaro, F. and Harris, D. E. (2012), Complex particle acceleration processes in the hotspots of 3C 105 and 3C 445, *Monthly Notices of the Royal Astronomical Society*, **419**(3), pp. 2338–2348.

Prieto, M. A., Brunetti, G. and Mack, K.-H. (2002), Particle accelerators in the hot spots of radio galaxy 3c 445, imaged with the vlt, *Science*, **298**(5591), pp. 193–195.